

Mobility edges and localization characteristics in one-dimensional quasiperiodic quantum walk

Xin-Hui Cui(崔鑫辉), Hui-Min Wang(王慧敏), and Zhi-Jian Li(李志坚)

Citation: Chin. Phys. B, 2024, 33 (**6**): 060301. DOI: 10.1088/1674-1056/ad342d
Journal homepage: http://cpb.iphy.ac.cn; http://iopscience.iop.org/cpb

What follows is a list of articles you may be interested in

Anomalous non-Hermitian dynamical phenomenon on the quantum circuit

Chenxiao Dong(董陈潇), Zhesen Yang(杨哲森), Jinfeng Zeng(曾进峰), and Jiangping Hu(胡江平)
Chin. Phys. B, 2023, 32 (**7**): 070305. DOI: 10.1088/1674-1056/acce9a

Efficient quantum private comparison protocol based on one direction discrete quantum walks on the circle

Jv-Jie Wang(王莒杰), Zhao Dou(窦钊), Xiu-Bo Chen(陈秀波), Yu-Ping Lai(赖裕平), and Jian Li(李剑)
Chin. Phys. B, 2022, 31 (**5**): 050308. DOI: 10.1088/1674-1056/ac5a3f

Quantum walk search algorithm for multi-objective searching with iteration auto-controlling on hypercube

Yao-Yao Jiang(姜瑶瑶), Peng-Cheng Chu(初鹏程), Wen-Bin Zhang(张文彬), and Hong-Yang Ma(马鸿洋)
Chin. Phys. B, 2022, 31 (**4**): 040307. DOI: 10.1088/1674-1056/ac2806

Disorder in parity-time symmetric quantum walks

Peng Xue(薛鹏)
Chin. Phys. B, 2022, 31 (**1**): 010311. DOI: 10.1088/1674-1056/ac3741

Quantum walk under coherence non-generating channels

Zishi Chen(陈子石) and Xueyuan Hu(胡雪元)
Chin. Phys. B, 2021, 30 (**3**): 030305. DOI: 10.1088/1674-1056/abd74d

---

Mobility edges and localization characteristics in one-dimensional quasiperiodic quantum walk

Xin-Hui Cui(崔鑫辉), Hui-Min Wang(王慧敏), and Zhi-Jian Li(李志坚)†

Institute of Theoretical Physics, State Key Laboratory of Quantum Optics and Quantum Devices, Shanxi University, Taiyuan 030006, *China*

(Received 8 January 2024; revised manuscript received 27 February 2024; accepted manuscript online 15 March 2024)

We construct a one-dimensional quasiperiodic quantum walk to investigate the localization–delocalization transition. The inverse participation ratio and Lyapunov exponent are employed as two indexes to determine the mobility edge, a critical energy to distinguish the energy regions of extended and localized states. The analytical solution of mobility edge is obtained by the Lyapunov exponents in global theory, and the consistency of the two indexes is confirmed. We further study the dynamic characteristics of the quantum walk and show that the probabilities are localized to some specific lattice sites with time evolution. This phenomenon is explained by the effective potential of the Hamiltonian which corresponds to the phase in the coin operator of the quantum walk.

Keywords: quantum walk, mobility edges, quasiperiodicity

PACS: 03.65.−w, 03.67. Lx, 05.60.Gg **DOI:** 10.1088/1674-1056/ad342d

1. Introduction

Quantum walk (QW) is the counterpart and generalization of classical random walk in the quantum scenario.[1–3] However, unlike the classical case, QW cannot be simply perceived as moving forward or backward. The principles of quantum mechanics, i.e., quantum superposition and interference, play significant roles in QW.[4,5] Many superior dynamical characteristics are exhibited, such as propagation speed being faster than classical random walk.

The system is influenced inevitably by impurities and disorders. Disorders generally can be classified into random disorders and quasiperiodic disorders. Anderson localization is caused by both disorders and has become an everlasting research topic.[6–9] Although the localization–delocalization transition is absent in low-dimensional random disorder systems,[10–13] it can occur even in one-dimensional (1D) quasiperiodic systems.[14–16] Moreover, in comparison with the random disorder systems, the quasiperiodic systems have advantages for exploring exact results due to the still existing beneficial transformation from position pace to momentum pace.

Most works on the localized effect induced by the quasi-periodicity focus on the systems described by Hamiltonian.[17–20] In fact, discrete-time QW as a stroboscopic simulator of an effective Hamiltonian can be equivalent to a Floquet system,[21,22] in which both 0-energy states and π-energy states appear in the band gap. Meanwhile, mobility edges now are regarded as an energy threshold that distinguishes the local state from the extended state,[23–29] which was originally used in electronic systems to describe the migration properties of electrons in irregular crystalline potential fields. In this paper, we study a 1D quasiperiodic QW and explore the precise solution of the mobility edges through the Lyapunov exponents (LE). Furthermore, the dynamic characteristics are discussed.

2. Model and mobility edge

We consider a quasiperiodic QW on 1D lattice. As shown in Fig. 1, each cell (green box) of the lattice includes two sites (black dot and yellow dot). A coin phase operator is applied on the even sites (yellow dots) and its action is equivalent to imposing a potential energy (yellow dashed curve) on the even sites in the Hamiltonian system.[30] The QW is defined in the direct product Hilbert space of position space $\{|x\rangle\}$ and coin space $\{|s\rangle, s=\uparrow,\downarrow\}$. The evolution operator of the QW in our model is

$$U = SP_2R(\theta)SP_1R(\theta), \tag{1}$$

where the conditional shift operator S is

$$S = \sum_x |x+1\rangle\langle x| \otimes |\uparrow\rangle\langle\uparrow| + |x-1\rangle\langle x| \otimes |\downarrow\rangle\langle\downarrow|, \tag{2}$$

and the coin operator R is implemented by SU (2) rotation operation

$$R(\theta) = \sum_x |x\rangle\langle x| \otimes \begin{pmatrix} \cos\theta & -\sin\theta \\ \sin\theta & \cos\theta \end{pmatrix}. \tag{3}$$

We let the phase operator P_1 and P_2 satisfy with the relation $P_2 = P_1^{-1}$, and P_1 is defined as

$$P_1 = \begin{cases} \sum_x |x\rangle\langle x| \otimes \begin{pmatrix} e^{\frac{i}{2}\pi\cos(x\pi\omega)} & 0 \\ 0 & e^{-\frac{i}{2}\pi\cos(x\pi\omega)} \end{pmatrix}, & x = 2m, \\ \sum_x |x\rangle\langle x| \otimes \begin{pmatrix} 1 & 0 \\ 0 & 1 \end{pmatrix}, & \text{otherwise}, \end{cases} \tag{4}$$

where $m = 1, 2, \ldots, N$ denotes the cell index on the lattice, and the total site number of the lattice is $L = 2N$. Equation (4)

†Corresponding author. E-mail: zjli@sxu.edu.cn

© 2024 Chinese Physical Society and IOP Publishing Ltd

means that the QW accumulates a phase factor at even sites while not at odd sites. The quasi-periodicity of the model is introduced by taking the value of parameter ω to be irrational. As a result, the phases accumulated on each site are different in spite of it is a cosine function of position.

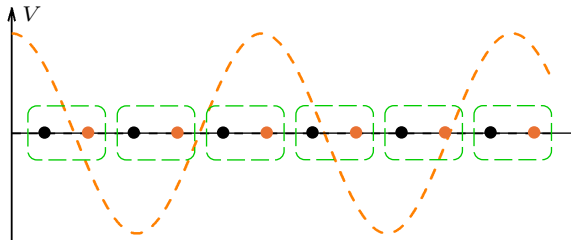


Fig. 1. Illustration of 1D lattice and the equivalent potential for the 1D quasi-periodic QW model.

In this paper, we focus on the study of extended or delocalized states of QW. The mobility edge is one of the most important concepts in quasiperiodic systems. It is an energy threshold that separates extended states from localized states. There are many indexes to determine the mobility edge. A commonly used one is the inverse participation ratio (IPR).[31,32] IPR of the nth eigenstate $|\psi_n\rangle$ is defined as

$$\mathrm{IPR}_n = \frac{\sum_{x=1}^{L} |\langle x|\psi_n\rangle|^4}{\left(\sum_{x=1}^{L} |\langle x|\psi_n\rangle|^2\right)^2}. \tag{5}$$

When the eigenstate is an extended state, especially the probabilities distribution is uniform over all lattice sites, i.e., $\langle x|\psi_n\rangle \sim 1/\sqrt{L}$, the IPR can be approximated to $1/L$. If the lattice is long enough, the IPR will tend to zero. On the other hand, when the eigenstate is a localized state, such as the extreme situations of all probabilities concentrating on a single site, the IPR will tend to 1.

The other commonly used index to determine the value of the mobility edge is the LE, which can be analytically obtained by the Avila's global theory of quasiperiodic Schrödinger operators. LE initially is used for depicting the stability of a dynamical system. Negative LE indicates instability of the system with extended eigenstates, while positive LE indicates stability of the system with localized eigenstates. Therefore, the energy at which the LE equals zero is referred to as the mobility edge. The LE can be expressed as[33]

$$\gamma(E) = \lim_{L\to\infty} \frac{1}{L} \ln \|\boldsymbol{T}_L(E)\|, \tag{6}$$

where $\|\cdot\|$ denotes the norm of the matrix and

$$\boldsymbol{T}_L(E) = \prod_{m=1}^{N} \boldsymbol{T}_m(E) \tag{7}$$

is the transfer matrix of the whole system under periodic boundary conditions. $\boldsymbol{T}_m$ is the transition matrix from the m-th cell to the $(m+1)$-th cell.

3. Result and discussion

We generally express the eigenfunction of the QW as

$$|\psi\rangle = \sum_{x,s} u_{x,s} |x\rangle \otimes |s\rangle, \tag{8}$$

which satisfies the eigen equation $U|\psi\rangle = \lambda|\psi\rangle$, and λ is the corresponding eigenvalue. The QW can be viewed as a stroboscopic simulation of the time evolution driven by an effective Hamiltonian H. That is to say that U and H have the relation $U = \mathrm{e}^{-\mathrm{i}H}$, so the eigenvalue λ and the effective eigenenergy E satisfy with $\lambda = \mathrm{e}^{\mathrm{i}E} = \cos E + \mathrm{i}\sin E$. From the eigen equation, we can obtain the linear equations

$$\begin{pmatrix} u_{x+2,\uparrow} \\ u_{x+2,\downarrow} \end{pmatrix} = \boldsymbol{T}_x \begin{pmatrix} u_{x,\uparrow} \\ u_{x,\downarrow} \end{pmatrix}, \tag{9}$$

complied by the expansion coefficients $u_{x,s}$ in Eq. (8). $\boldsymbol{T}_x$ are the transfer matrix between odd/even sites in adjacent cells and their expressions are

$$\boldsymbol{T}_{\mathrm{odd}} = \begin{pmatrix} \dfrac{1}{\lambda} & -\dfrac{(\lambda+1)\sin\theta}{\lambda\cos\theta} \\ -\dfrac{(\lambda+1)\sin\theta}{\lambda\cos\theta} & \dfrac{(\lambda+\sin\theta)^2}{\lambda\cos^2\theta} \end{pmatrix}, \tag{10}$$

and

$$\boldsymbol{T}_{\mathrm{even}} = \begin{pmatrix} \dfrac{1}{\lambda} & -\dfrac{\left(\lambda\,\mathrm{e}^{-\mathrm{i}\pi\cos(2m\pi\omega)}+1\right)\sin\theta}{\lambda\cos\theta} \\ -\dfrac{\left(\lambda\,\mathrm{e}^{\mathrm{i}\pi\cos(2m\pi\omega)}+1\right)\sin\theta}{\lambda\cos\theta} & \dfrac{\left(\sin\theta+\lambda\,\mathrm{e}^{-\mathrm{i}\pi\cos(2m\pi\omega)}\right)\left(\sin\theta+\lambda\,\mathrm{e}^{\mathrm{i}\pi\cos(2m\pi\omega)}\right)}{\lambda\cos^2\theta} \end{pmatrix}, \tag{11}$$

for odd sites and even sites, respectively. Because the couplings only occur between the odd/even sites in adjacent cells, but not between the odd site and even site, the transfer matrix between adjacent cells can be defined by merging $\boldsymbol{T}_{\mathrm{odd}}$ and $\boldsymbol{T}_{\mathrm{even}}$ to be as

$$\boldsymbol{T}_m = \begin{pmatrix} \boldsymbol{T}_{\mathrm{even}} & 0 \\ 0 & \boldsymbol{T}_{\mathrm{odd}} \end{pmatrix}. \tag{12}$$

Substituting Eq. (12) into Eq. (6) and letting $\gamma(E) = 0$, we ob-

tain

$$\begin{aligned}&\left|\lambda^3(\cos^4\theta+\sin^2\theta\cos\theta+\cos\theta\sin\theta+\sin^2\theta+\cos^3\theta)\right.\\&+\lambda^2(2\sin^2\theta+\sin\theta+\sin^4\theta+1+\cos^3\theta)+\cos^3\theta\sin^2\theta\\&\left.+\lambda\sin^3\theta\cos\theta+\cos^4\theta\right|^2=|\lambda|^2\cos^4\theta.\end{aligned}\tag{13}$$

It should be pointed out that the above equation is independent of parameters ω. The reason is that the phase factor $\mathrm{e}^{\mathrm{i}\pi\cos(2m\pi\omega)}$ plays no role in finding the norm of $\boldsymbol{T}_m$ according to Eq. (6). Solving the above equation and using $\lambda=\mathrm{e}^{\mathrm{i}E}=\cos E+\mathrm{i}\sin E$, we finally obtain the mobility edges E_c as

$$\begin{aligned}E_\mathrm{c}=\pm\arccos\Bigg[&\frac{\cos^4\theta+\cos^2\theta\sin^2\theta+3+4\sin^2\theta}{5\sin^3\theta-2\cos\theta\sin\theta-\cos^4\theta\sin^4\theta-4\cos^2\theta\sin\theta-2\cos\theta\sin^2\theta}\\&+\frac{2\cos^2\theta\sin^4\theta-3\sin^4\theta-2\cos^4\theta\sin^2\theta+2\cos^4\theta\sin^4\theta}{5\sin^3\theta+2\cos\theta\sin\theta+\cos^4\theta\sin^4\theta-4\cos^2\theta\sin\theta-2\cos\theta\sin^2\theta}\Bigg].\end{aligned}\tag{14}$$

Next, we numerically calculate the eigenproblem of U in Eq. (1) to study IPR. For quasiperiodic systems, we assume $\omega=(\sqrt{5}-1)/2=\lim\limits_{n\to\infty}(F_{n-1}/F_n)$ (the golden mean), where F_n are the Fibonacci numbers defined recursively by $F_{n+1}=F_n+F_{n-1}$ and $F_0=F_1=1$. Figure 2 shows the variation of real components of the eigenenergy spectra with increasing parameter θ, where $L=200$ is taken and the periodic boundary condition is applied. The colors in Fig. 2 represent the IPR of the corresponding eigenstates. As a comparison, the real components of mobility edges E_c in Eq. (14) are plotted by the black curve. It is shown that both the analytical mobility edge from LE and the numerical critical values from IPR can characterize the localization–delocalization transition. The consistency of the two indexes is confirmed. For given θ, when the eigenenergy is less than the mobility edge, IPR $\approx 1/L$ and the corresponding eigenstate is an extended state. On the other hand, when the eigenenergy is greater than the mobility edge, IPR $\to 1$ and the eigenstate is a localized state. It needs to be pointed out that when ω is a rational number, the LE can not work as an indicator of the mobility edge. However, the IPR can still distinguish between located and extended behaviors. For such cases, all the eigenstates are extended states and IPR $\to 0$.

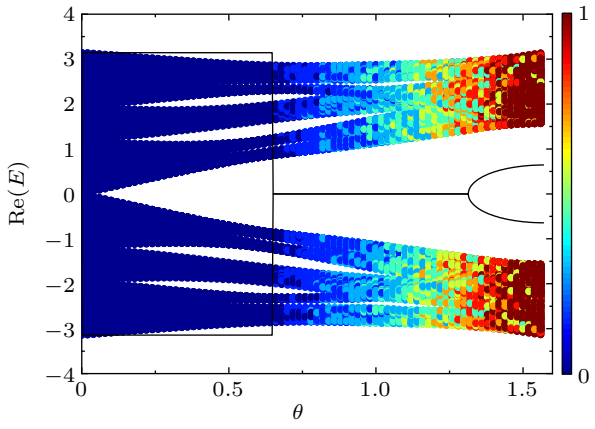


Fig. 2. The real components of the eigenenergy E, colored according to the IPR of corresponding eigenstates.

For further understanding the localized and extended behaviors of QW, we analyze its dynamical evolution under the irrational parameter ω. If not otherwise specified, we always take $\omega=(\sqrt{5}-1)/2$ in the following numerical calculation. QW as a stroboscopic simulator is driven by the Floquet operator U, which repeatedly acts on the initial state $|\psi_0\rangle$. The wave function after t time steps is given by $|\psi(t)\rangle=U^t|\psi_0\rangle$ and so the probability of finding the walker at site x is

$$p(x,t)=\sum_{s=\uparrow,\downarrow}|\langle s,x|\psi(t)\rangle|^2,\tag{15}$$

when $\theta=\pi/8$, we take the localized initial state

$$|\psi_0\rangle=|x_0=50\rangle\otimes\frac{1}{\sqrt{2}}(|\uparrow\rangle+\mathrm{i}\,|\downarrow\rangle),$$

and the uniformly extended initial state

$$|\psi_0\rangle=\left[\frac{1}{\sqrt{L}}\sum_{j=1}^{L}|j\rangle\right]\otimes\left[\frac{1}{\sqrt{2}}(|\uparrow\rangle+\mathrm{i}\,|\downarrow\rangle)\right]$$

to plot the dynamical probability distribution of QW in Figs. 3(a) and 3(b), respectively. It is shown that the probabilities distribute over all lattice sites with time evolution regardless of the initial state being a localized state or an extended state. Correspondingly, the IPR is vanishingly small in Fig. 2 when $\theta=\pi/8$, the eigenstates of QW are all extended states.

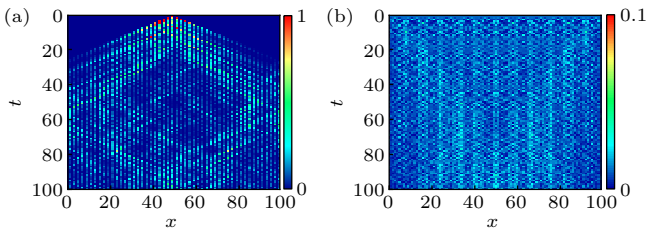


Fig. 3. The dynamical probability distribution of QW with $\theta=\pi/8$. (a) The localized initial state and (b) the extended initial state.

When $\theta=3\pi/8$, the IPR is finite so the eigenstates of the QW are localized states. For such cases, the probability distribution $p(x,t)$ always localizes at certain sites and the localized sites can be determined by the effective site potential. The quasiperiodicity of QW is introduced through the phase

operator $P_{1,2}$ with the irrational parameter ω. The phase operator can be understood as a quasiperiodic site potential of effective Hamiltonian,[30] which is

$$V(x) = \begin{cases} \cos(x\pi\omega)\pi, & x \text{ is even}, \\ 0, & x \text{ is odd}. \end{cases} \tag{16}$$

The variation of quasiperiodic potential with the position is plotted in Fig. 4. At the odd sites, the quasiperiodic potential is zero. When the zero value is a minimum of the valley, the corresponding site coordinates are marked on the horizontal axis by the green dashed line. When the zero value is a peak and the potential on its neighboring even sites is the minimum of the valley, the corresponding even site coordinates are marked by the yellow dashed line. We will see in the following that these marked coordinate positions are the bunching positions of the probability distribution for different initial states.

We choose the initial state of QW starting from one site $|x_0\rangle$ and the coin state is a symmetry distribution state $|s\rangle = (1/\sqrt{2})(|\uparrow\rangle + \mathrm{i}\,|\downarrow\rangle)$. When $x_0 = 39$, 47, 53 marked by the green triangle in the Fig. 4, the probability distributions with the time evolution are shown in Figs. 5(a)–5(c). One common characteristic can be observed that the probability will eventually localize to the site $x = 47$. This is because the site of

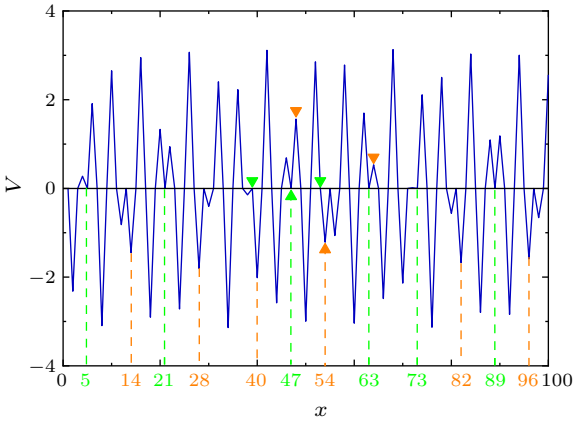


Fig. 4. The variation of the quasiperiodic potential V with the lattice site x.

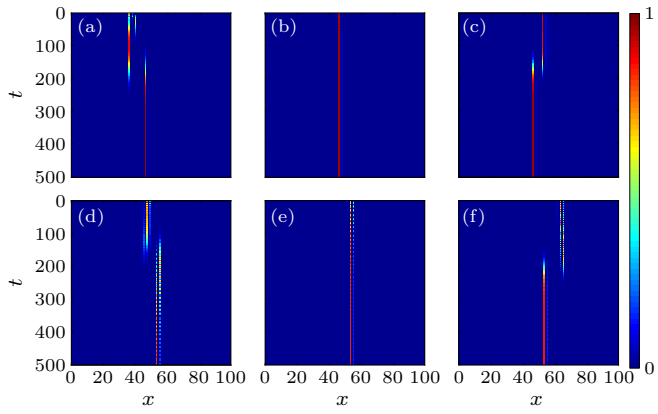


Fig. 5. The dynamical probability distribution of QW for $\theta = 3\pi/8$ and (a) $x_0 = 39$, (b) $x_0 = 47$, (c) $x_0 = 53$, (d) $x_0 = 48$, (e) $x_0 = 54$, (f) $x_0 = 64$. The other parameters are the same as in Fig. 3.

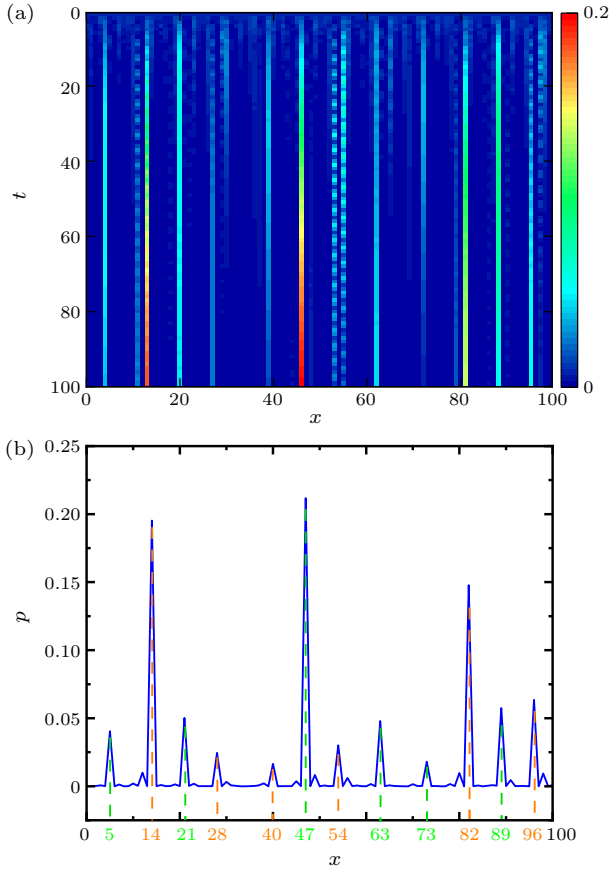


Fig. 6. (a) Dynamical probability distribution of QW with initial state being uniformly distributed on each site. (b) The plane display of panel (a) at $t = 100$ steps. The other parameters are the same as in Fig. 5.

$x = 47$, as one of the zero potential sites and the minimums of the potential valley, is the closest to these starting sites. More generally, when QW starts from the odd sites, the probability distribution ultimately localizes at the closest sites where the potential value is zero and the minimum of the potential valley. As mentioned above, these sites are $x = 5$, 21, 47, 63, 73, 89 marked by the green dashed line in Fig. 4. On the other hand, when QW starts from the even sites, the probability distribution with time evolution ultimately localizes the sites marked by the yellow dashed line in Fig. 4, where potential value is a minimum of the potential valley and the potential at one of its neighboring odd sites is a peak with zero value. For instance, Figs. 5(d)–5(f) show the probability distribution with time evolution localized to the site $x = 54$ when we take $x_0 = 48$, 54, 64 marked by the yellow triangle in Fig. 4. Each step of time evolution includes two conditional shift operators, so when QW starts from the odd (even) site, it only reaches the odd (even) sites with the time evolution. The quasiperiodic potential induces QW to localize to the nearest one of the sites indicated by the green or yellow lines in Fig. 4. Especially, if we consider QW to be uniformly distributed on each site at the initial moment, i.e., the initial state of QW is

$$|\psi_0\rangle = \left[\frac{1}{\sqrt{L}}\sum_{j=1}^{L}|j\rangle\right] \otimes \left[\frac{1}{\sqrt{2}}(|\uparrow\rangle + \mathrm{i}\,|\downarrow\rangle)\right],$$

it is predictable that the probability distribution will evolve into the strip pattern as shown in Fig. 6(a). After $t = 100$ steps, the probabilities on each site are presented in Fig. 6(b). As expected, the sites corresponding to the peaks of probability distribution are as same as those marked by green and yellow dashed lines in Fig. 4. Particularly, we change ω to be $\omega = \sqrt{2} - 1$ (the silver mean) and $\omega = (\sqrt{13} - 3)/2$ (the bronze mean), the above dynamical results are unchanged .

4. Conclusion

We construct a 1D quasiperiodic QW and study its localized characteristics. The quasiperiodicity is introduced through the coin phase operator with irrational parameters, which can be understood as a quasiperiodic potential of the effective Hamiltonian. Quasiperiodicity induces localization–delocalization phenomena and the mobility edge is calculated through two indexes IPR and LE. For given θ, the eigenstates of QW are extended states when the corresponding eigenenergies are less than the mobility edge, otherwise, they are localized states. We further analyze the dynamical probability distribution for different initial states to discuss the localization. The localized sites can be determined by the effective Hamiltonian potential from the coin phase operator of the QW. Generally, when QW starts from the odd sites, the probability localizes at the odd sites where the potential values are zero and the minimum of the valley. When QW starts from the even sites, the probability eventually localizes the even sites where the potential value is a minimum of the potential valley and the potential at one of its neighboring odd sites is a peak with zero value. The solvability of our model provides a new playground to analyze and explore the richness of localization phenomena.

References

[1] Aharonov Y, Davidovich L and Zagury N 1993 *Phys. Rev. A* **48** 1687
[2] Kempe J 2003 *Contemp. Phys.* **44** 307
[3] Venegas-Andraca S E 2012 *Quantum Inf. Process.* **11** 1015
[4] Childs A M 2009 *Phys. Rev. Lett.* **102** 180501
[5] Kitagawa T, Berg E, Rudner M and Demler E 2010 *Phys. Rev. B* **82** 235114
[6] Anderson P W 1958 *Phys. Rev.* **109** 1492
[7] Mochizuki K, Kim D and Obuse H 2016 *Phys. Rev. A* **93** 062116
[8] Bender C M and Boettcher S 1998 *Phys. Rev. Lett.* **80** 5243
[9] Zhou H and Lee J Y 2019 *Phys. Rev. B* **99** 235112
[10] Zhang K, Yang Z and Fang C 2020 *Phys. Rev. Lett.* **125** 126402
[11] Yao S and Wang Z 2018 *Phys. Rev. Lett.* **121** 086803
[12] Hatano N and Nelson D R 1996 *Phys. Rev. Lett.* **77** 570
[13] Hatano N and Nelson D R 1998 *Phys. Rev. B* **58** 8384
[14] Kolesnikov A V and Efetov K B 2000 *Phys. Rev. Lett.* **84** 5600
[15] Gong Z, Ashida Y, Kawabata K, Takasan K, Higashikawa S and Ueda M 2018 *Phys. Rev. X* **8** 031079
[16] Harper P G 1955 *Proc. Phys. Soc. A* **68** 874
[17] Liu Y, Wang Y, Liu X J, Zhou Q and Chen S 2021 *Phys. Rev. B* **103** 014203
[18] Liu Y, Wang Y, Zheng Z and Chen S 2021 *Phys. Rev. B* **103** 134208
[19] Longhi S 2021 *Phys. Rev. B* **103** 054203
[20] Acharya A P, Chakrabarty A, Sahu D K and Datta S 2022 *Phys. Rev. B* **105** 014202
[21] Lin Q, Li T, Xiao L, Wang K, Yi W and Xue P 2022 *Nat. Commun.* **13** 3229
[22] Xiao L, Deng T, Wang K, Wang Z, Yi W and Xue P 2021 *Phys. Rev. Lett.* **126** 230402
[23] Wang Y, Xia X, Zhang L, Yao H, Chen S, You J, Zhou Q and Liu X J 2020 *Phys. Rev. Lett.* **125** 196604
[24] Wang Y, Zhang L, Wan Y, He Y and Wang Y 2023 *Phys. Rev. B* **107** L140201
[25] Jiang H, Lang L J, Yang C, Zhu S L and Chen S 2019 *Phys. Rev. B* **100** 054301
[26] Xiong Y 2018 *J. Phys. Commun.* **2** 035043
[27] Martinez Alvarez V M, Barrios Vargas J E and Foa Torres L E F 2018 *Phys. Rev. B* **97** 121401
[28] Guo C X, Liu C H, Zhao X M, Liu Y and Chen S 2021 *Phys. Rev. Lett.* **127** 116801
[29] Liu Y, Zeng Y, Li L and Chen S 2021 *Phys. Rev. B* **104** 085401
[30] Li Z J, Izaac J A and Wang J B 2013 *Phys. Rev. A* **87** 012314
[31] Schreiber M 1985 *J. Phys. C: Solid State Phys.* **18** 2493
[32] Wegner F 1980 *Z. Physik B* **36** 209
[33] Lin X, Chen X, Guo G C and Gong M 2023 *Phys. Rev. B* **108** 174206